

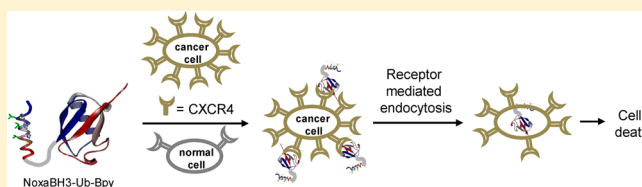
## Targeted Delivery of Ubiquitin-Conjugated BH3 Peptide-Based Mcl-1 Inhibitors into Cancer Cells

Avinash Muppidi,<sup>†</sup> Kenichiro Doi,<sup>‡</sup> Selvakumar Edwardraja,<sup>†</sup> Surya V. S. R. K. Pulavarti,<sup>†</sup> Thomas Szyperski,<sup>†</sup> Hong-Gang Wang,<sup>\*,‡</sup> and Qing Lin<sup>\*,†</sup>

<sup>†</sup>Department of Chemistry, State University of New York at Buffalo, Buffalo, New York 14260-3000, United States

<sup>‡</sup>Department of Pharmacology, Pennsylvania State University College of Medicine, Hershey, Pennsylvania 17033, United States

**ABSTRACT:** BH3 peptides are key mediators of apoptosis and have served as the lead structures for the development of anticancer therapeutics. Previously, we reported the application of a simple cysteine-based side chain cross-linking chemistry to NoxaBH3 peptides that led to the generation of the cross-linked NoxaBH3 peptides with increased cell permeability and higher inhibitory activity against Mcl-1 (Muppidi, A., Doi, K., Edwardraja, S., Drake, E. J., Gulick, A. M., Wang, H.-G., Lin, Q. (2012) *J. Am. Chem. Soc.* 134, 14734). To deliver cross-linked NoxaBH3 peptides selectively into cancer cells for enhanced efficacy and reduced systemic toxicity, here we report the conjugation of the NoxaBH3 peptides with the extracellular ubiquitin, a recently identified endogenous ligand for CXCR4, a chemokine receptor overexpressed in cancer cells. The resulting ubiquitin-NoxaBH3 peptide conjugates showed increased inhibitory activity against Mcl-1 and selective killing of the CXCR4-expressing cancer cells. The successful delivery of the NoxaBH3 peptides by ubiquitin into cancer cells suggests that the ubiquitin/CXCR4 axis may serve as a general route for the targeted delivery of anticancer agents.



### INTRODUCTION

During the past two decades, there has been increasing interest in developing biologics-based therapeutics, including therapeutic enzymes, monoclonal antibodies, and peptides. Among the biologics, peptides have lowest molecular weight and can be readily optimized to possess drug-like properties.<sup>1</sup> There are currently more than 40 peptide drugs approved for clinical use, the majority of which bind to the extracellular targets because of their inefficient cell permeability. To allow peptides to access the intracellular targets, two approaches have been developed recently: (1) conjugation to the cell-penetrating peptides such as HIV-tat, oligoarginine, and Pep-1<sup>2,3</sup> and (2) chemical modifications to stabilize the secondary structures and optimize the physicochemical properties.<sup>4–6</sup> While these approaches have improved the intracellular uptake, the nonspecific uptake of the peptides into both normal cells and cancer cells reduces their therapeutic windows.<sup>7–9</sup> Thus, it is highly desirable that the peptide drugs are selectively delivered to tumor cells to maximize their efficacy while reducing systemic toxicity. To date, strategies for targeted cancer drug delivery have relied on the differences in cellular compositions between normal cells and cancer cells. Indeed, the use of RGD peptides,<sup>10</sup> proteins,<sup>11</sup> and antibodies<sup>12</sup> to target the upregulated receptors in tumor environment for selective drug delivery has gained momentum recently. In this work, we explored the use of extracellular ubiquitin, a natural ligand for CXCR4,<sup>13</sup> a chemokine receptor overexpressed in cancer cells, as a delivery vehicle for peptide-based anticancer drugs.

Extracellular ubiquitin has been known to have immunomodulatory and anti-inflammatory properties for many years.<sup>14,15</sup>

However, the mechanism of these effects was only identified very recently. Extracellular ubiquitin was found to be a natural ligand of CXCR4,<sup>13</sup> which plays a major role in cancer cell chemotaxis and is expressed in many tumors including multiple myeloma, AML, prostate cancer, breast cancer, and ovarian cancer.<sup>16</sup> The expression level of CXCR4 was found to correlate with the aggressiveness of the cancer.<sup>17</sup> Extracellular ubiquitin, once it has entered cells via CXCR4-mediated endocytosis, was found to be conjugated with the intracellular proteins, indicating its endosomal release.<sup>18</sup> On the basis of these observations, we hypothesize that the ubiquitin/CXCR4 axis may offer a novel route for targeted cytosolic delivery of peptide drugs into tumor cells. We have recently reported a new side chain cross-linking chemistry to reinforce helical peptides and increase their cellular uptake<sup>19</sup> and applied this chemistry to the design of the cell-permeable cross-linked NoxaBH3 peptides as potent and selective Mcl-1 inhibitors.<sup>20</sup> Herein, we report the preparation of the cross-linked NoxaBH3 peptide–ubiquitin conjugates, the characterization of their inhibitory activities against Mcl-1, the study of their uptake mechanism, and the determination of their cell-killing activities against the CXCR4-positive cells, and the investigation of their proteolytic stability in fresh mouse serum. To our knowledge, this study represents the first example of exploiting the ubiquitin/CXCR4 axis for targeted delivery of cancer therapeutics.

**Received:** December 3, 2013

**Revised:** January 7, 2014

**Published:** January 11, 2014

## EXPERIMENTAL SECTION

**General Methods.** 6,6'-Bis-bromomethyl-[3,3']bipyridine (Bpy) was prepared using the procedure described previously.<sup>19</sup> Rabbit antiubiquitin antibody was purchased from Thermo Scientific, and rabbit anti-His<sub>6</sub> antibody was purchased from Rockland Immunochemicals. Mouse anti-CXCR4 antibody was purchased from R&D Systems. LC-MS was performed using a Finnigan LCQ Advantage IonTrap mass spectrometry coupled with a Surveyor HPLC system. Protein liquid chromatography was run on a Phenomenex Jupiter C4 column (5  $\mu$ m, 300 Å, 2.00  $\times$  50 mm<sup>2</sup>) with a flow rate of 250  $\mu$ L/min and a linear gradient of 5–95% acetonitrile/H<sub>2</sub>O containing 0.1% formic acid over 30 min.

**Construction of the Ubiquitin-BH3 Peptide Conjugates.** The synthetic, codon-optimized genes encoding the ubiquitin–peptide conjugates in pUC57 were purchased from GenScript (Piscataway, NJ). The PU fragments were ligated into the *NdeI/XhoI* sites in the pET28a vector, while the UP fragment was ligated into the *NcoI/XhoI* sites in the pET28a vector. The resulting plasmids, pET28a-PU, pET28a-UP, and pET28a-PU-KKmt, were verified by DNA sequencing. For protein expression, BL21(DE3) cells bearing appropriate expression plasmids were allowed to grow in 1 L LB medium containing 50  $\mu$ g/mL kanamycin at 37 °C to OD<sub>600</sub> 0.6. Then, 0.5 mM isopropyl- $\beta$ -D-thiogalactopyranoside was added to the culture to induce protein expression for an additional 6 h. The cells were harvested by centrifugation, and the cell pellets were resuspended in 20 mL of binding buffer (50 mM Na<sub>2</sub>HPO<sub>4</sub> and 300 mM NaCl, pH 8.0) containing 10 mM imidazole and lysed by passing the cell suspension through a French press. The lysates were centrifuged at 16,000 rpm for 30 min, and the supernatants were filtered through a 0.2  $\mu$ m filter first before applying them to a column packed with 0.4 mL of Ni-NTA beads pre-equilibrated with PBS buffer containing 2 mM DTT. The beads were washed with 20 mL of washing buffer containing 50 mM imidazole, and the protein conjugates were eluted with 2 mL of elution buffer containing 250 mM imidazole. The protein concentrations were determined by the Bradford assay.

**Cross-Linking Reaction with the Ubiquitin–Peptide Conjugates.** The purified protein was subjected to buffer-exchange into 50 mM ammonium bicarbonate containing 5 mM EDTA, pH 8.5, using a 3,000 MW cutoff Amicon Ultra (Fisher Scientific) centrifugal filter unit and concentrated to 1 mg/mL. The solution was treated with an equal volume of immobilized TCEP disulfide reducing gel (Thermo Scientific) for 2 h before incubating with 5 equiv of Bpy in 30% acetonitrile/50 mM ammonium bicarbonate buffer, pH 8.5, for 2 h. Afterward, excess reagents were removed through buffer exchange to yield the Bpy-cross-linked ubiquitin–peptide conjugates, which were then used directly in subsequent studies without further purification.

**Fluorescence Polarization Assay.** The FITC-labeled Bim-BH3 peptide (DMRPEIWIQAQLRRIGDEFNAYAR) was used in determining the inhibitory activities of the conjugates against Mcl-1. In brief, 20  $\mu$ L of 20 nM GST-tagged mouse Mcl-1(152–309) in PBS containing 0.005% Tween-20 was mixed with 5  $\mu$ L of the protein conjugates at the various concentrations in PBS containing 25% DMSO and 0.005% Tween-20 in the wells of a 96-well black polystyrene plate (Corning #3993). Then, 25  $\mu$ L of 10 nM FITC-Bim-BH3 in PBS containing 5% DMSO and 0.005% Tween-20 was added

to each well, and the mixtures were thoroughly mixed at 1450 rpm for 3 min with a BioShake IQ Thermo Mixer (QUANTIFOIL Instruments GmbH) at room temperature. The fluorescence polarization values in millipolarization (mP) units were measured for 0.2 s at excitation and emission wavelengths of 480 and 535 nm, respectively, using a PerkinElmer 2030 multilabel plate reader. IC<sub>50</sub> was determined by fitting the data to a sigmoidal dose–response nonlinear regression model using SigmaPlot 10.0.1.  $K_i$  values were then calculated using the equation:  $K_i = [I]_{50}/([L]_{50}/K_d + P_0/K_d + 1)$ , where  $I_{50}$  and  $L_{50}$  are the free concentrations of the inhibitor and ligand, respectively, at 50% inhibition,  $P_0$  is the free concentration of protein in the absence of inhibitor, and  $K_d$  is the disassociation constant of the Bim:GST-Mcl-1 complex and has a value of 12.4 nM.

**NMR Sample Preparation and Data Acquisition.** Uniformly <sup>15</sup>N- and 5% biosynthetically directed fractionally <sup>13</sup>C-labeled PU-KKmt was expressed in BL21(DE3) cells in M9 minimal media using <sup>15</sup>NH<sub>4</sub>Cl (Cambridge Isotope Laboratories) and a mixture of 95% natural abundance and 5% *U*-<sup>13</sup>C-glucose (Sigma-Aldrich) as a carbon source in the culture medium, and purified using a Ni-NTA column. The identity of the [5% <sup>13</sup>C; *U*-<sup>15</sup>N]-labeled protein was confirmed by SDS–PAGE and LC-MS. The protein was then subjected to the cross-linking reaction under the same conditions as described earlier to generate [5% <sup>13</sup>C; *U*-<sup>15</sup>N]-PU-KKmt-Bpy. For NMR sample preparation, the proteins were dissolved at concentrations of 200  $\mu$ M in 10 mM sodium phosphate buffer (pH 6.0) containing 2 mM DTT, 0.02% sodium azide, and 10% D<sub>2</sub>O. 2D [<sup>15</sup>N,<sup>1</sup>H] heteronuclear single-quantum coherence (HSQC) spectra were acquired at 25 °C on an Agilent DDR 600 MHz spectrometer equipped with a <sup>1</sup>H{<sup>15</sup>N,<sup>13</sup>C} cryogenic probe. The spectra for PU-KKmt and PU-KKmt-Bpy were collected, respectively, with 128  $\times$  1024 complex points along  $t_1$  and  $t_2$  ( $t_{1,max}$  = 67 ms and  $t_{2,max}$  = 136 ms) in 1.5 h, and 256  $\times$  1024 complex points ( $t_{1,max}$  = 146 ms and  $t_{2,max}$  = 136 ms) in 2 h. For comparison, a 2D [<sup>15</sup>N,<sup>1</sup>H]-HSQC spectrum was recorded for a 1 mM [*U*-<sup>13</sup>C,<sup>15</sup>N]-labeled human ubiquitin sample in the same NMR buffer with 128  $\times$  1024 complex points ( $t_{1,max}$  = 60 ms and  $t_{2,max}$  = 136 ms) in 0.5 h. The spectra were processed using the program PROSA<sup>21</sup> and analyzed using the program CARRA.<sup>22</sup>

**Cellular Uptake Assay.** K562, Jurkat, or U937 cells were seeded in 10-cm dishes at appropriate densities in RPMI 1640 supplemented with 10% FBS, and incubated at 37 °C in a 5% CO<sub>2</sub> incubator overnight. On the next day, cells were washed with PBS, and the medium was switched to Opti-MEM. For temperature-dependency studies, Jurkat cells were incubated with 500  $\mu$ M PU-KKmt or PU-KKmt-Bpy at 37 or 4 °C for 2 h, treated with trypsin-EDTA for 15 min to remove surface-bound ubiquitin–peptide conjugates,<sup>23</sup> and lysed with 50  $\mu$ L of lysis buffer (50 mM HEPES, 50 mM NaCl, 10 mM Na<sub>2</sub>P<sub>4</sub>O<sub>7</sub>, 50 mM NaF, 1% Triton-X100, 5 mM EDTA, 1 mM sodium orthovanadate, and 0.5  $\mu$ L of Calbiochem protease inhibitor cocktail Set III) for 30 min on ice before proceeding to the Western blot assay. For competition assays, Jurkat cells in Opti-MEM medium were divided into 4 wells. One well was incubated with anti-CXCR4 antibody (R&D Systems, 20  $\mu$ g/mL), and the other three wells were incubated with ubiquitin at a concentration of 12.5, 25, and 50  $\mu$ M for 30 min. Afterward, cells were treated with 500 nM PU-KKmt-Bpy for 2 h. The cells were washed with PBS (3 $\times$ ) followed by treatment with 50  $\mu$ L of trypsin-EDTA (2.5 mg/mL in DMEM) for 15 min at 37 °C.

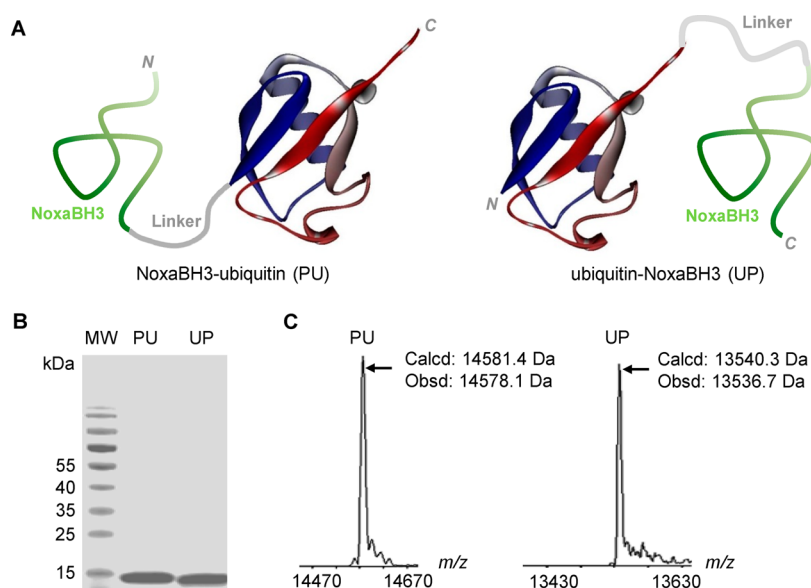


**Figure 1.** (A) Schematic structural representation of the ubiquitin–NoxaBH3 peptide conjugates with two different configurations. The mouse NoxaB-(68–93)-C75A sequence, a selective Mcl-1 inhibitor,<sup>31</sup> was used in the fusion along with (GGGGS)<sub>3</sub> as a flexible linker. (B) Coomassie Blue stained SDS–PAGE gel of the purified NoxaBH3–ubiquitin (PU) and ubiquitin–NoxaBH3 (UP) conjugates. (C) Deconvoluted masses of the PU and UP conjugates.

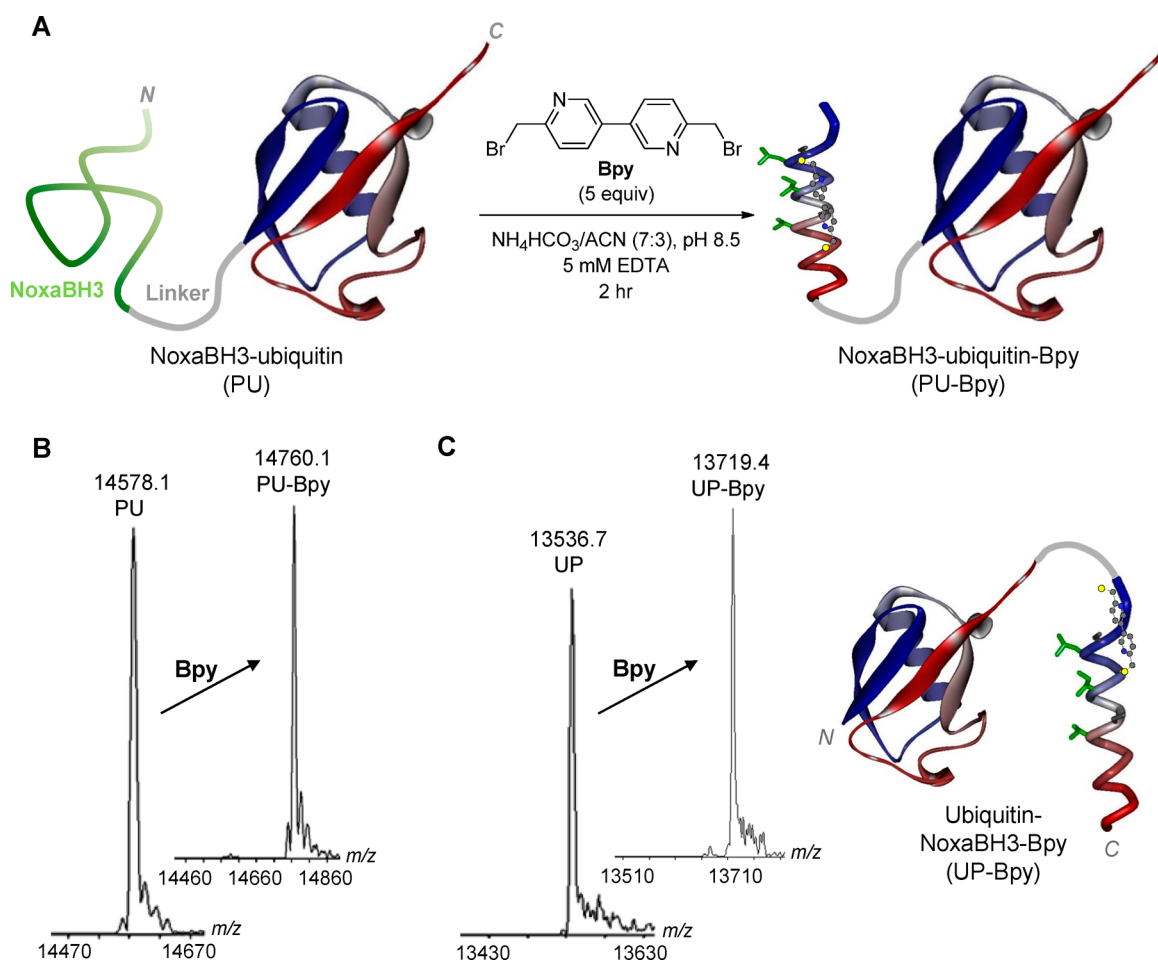


**Figure 2.** (A) Reaction scheme for the Bpy-mediated cross-linking of the NoxaBH3–ubiquitin conjugate. Bpy is rendered in a ball-and-stick model in the Bpy-cross-linked conjugate. (B,C) Deconvoluted masses of NoxaBH3–ubiquitin-Bpy (PU-Bpy) and analogous ubiquitin–NoxaBH3-Bpy (UP-Bpy).

The cells were washed again with PBS (3×) and lysed with 50  $\mu\text{L}$  of lysis buffer on ice for 30 min followed by centrifugation. The proteins in the supernatant were resolved by 4–12% Bis-Tris SDS–PAGE and transferred to a PDVF membrane. The membrane was blocked with 0.5% casein containing 0.1% Tween for 1 h, cut into two pieces, and probed separately using anti-His<sub>6</sub> antibody (Abgent, 1:2000 dilution) and anti- $\beta$ -actin antibody (Rockland Immunochemicals, 1:1000 dilution) as primary antibodies, and antimouse IgG-AP as secondary antibody (1:5000 dilution). The membrane was stained by incubating with the BCIP/NBT liquid substrate (Sigma-Aldrich), and the band intensities were quantified with ImageJ.

**Cell Viability Assay.** The cells in Opti-MEM medium were seeded into a 96-well plate at a density of  $10^4$  per well for K562 cells and  $10^5$  per well for U937 and Jurkat cells, treated with ubiquitin–NoxaBH3 peptide conjugates for 24 h, and the percentage of viable cells was quantified using the CellTiter 96 AQueous One Solution Cell Proliferation Assay kit (Promega) by following the manufacturer's recommended procedure.

**Serum Stability Assay.** The ubiquitin–peptide conjugates were added to fresh mouse serum (Equitech-Bio) to a final concentration of 25  $\mu\text{M}$ . The mixtures were incubated at 37 °C for 4 h. The 2  $\mu\text{L}$  aliquots were taken at 0, 2, and 4 h, and diluted into 100  $\mu\text{L}$  of PBST (PBS containing 0.05% Tween-20). The samples were flash frozen immediately and stored for ELISA. To a glutathione coated 96-well microtiter plate (Thermo Scientific) was added GST-Mcl-1 (200  $\mu\text{L}$ /well and 30  $\mu\text{g}/\text{mL}$  in PBS), and the plate was gently shaken at 4 °C overnight. After washing with PBST, the plate was blocked with 0.5% casein in PBST for 1 h. After washing with PBST (3×), the mouse serum-treated ubiquitin–peptide conjugates were added to each well and incubated for 2 h. Afterward, the wells were washed with PBST (3×), and the bound peptide–ubiquitin conjugates in each well were detected by incubating with 100  $\mu\text{L}$  of rabbit antiubiquitin antibody (1:1000 dilution) or rabbit anti-His<sub>6</sub> antibody (1:1000 dilution) for 1 h followed by antirabbit IgG-AP (1:1000 dilution) for 2 h. After washing with PBST (3×), 100  $\mu\text{L}$  DuoLux chemiluminescent and fluorescent alkaline phosphatase substrate solution (Vector Laboratories) were added, and the chemiluminescence signals were recorded by exposing the membrane to X-ray film in a dark room.

## RESULTS AND DISCUSSION

### Preparation of the Ubiquitin-BH3 Peptide Conjugates.

In exploiting the ubiquitin/CXCR4 axis for targeted delivery of the NoxaBH3 peptide-based Mcl-1 inhibitors, we had the following considerations: (1) the fusion of NoxaBH3 peptide to ubiquitin should not interfere with ubiquitin binding to CXCR4; and (2) the conjugation of ubiquitin to NoxaBH3 peptides should not negatively affect NoxaBH3 binding to Mcl-1. Accordingly, we fused the NoxaBH3 peptide at either the N- or the C-terminus of ubiquitin separated by a long flexible linker (GGGG)<sub>3</sub> (Figure 1A) to ensure that the two domains function properly. Thus, synthetic genes encoding the fusion proteins were inserted into the pET28a expression vector, and the His-tagged ubiquitin–peptide conjugates, NoxaBH3 peptide–ubiquitin (PU) and ubiquitin–NoxaBH3 peptide (UP), were purified to homogeneity with Ni-NTA-based affinity chromatography. SDS–PAGE and mass spectrometry analyses confirmed the identity and high purity of the conjugates (Figure 1B–C). Since the internalized extracellular ubiquitin may

**Table 1.** LC/ESI-MS Characterization of the Ubiquitin–NoxaBH3 Peptide Conjugates

name	sequence	mass calculated m/z	mass observed <sup>a</sup> m/z	% conversion <sup>b</sup>
NoxaBH3–ubiquitin (PU)	MGSSHHHHSSGLVPRGSHMPADLKDEAA $\underline{\text{C}}$ LRIGDCVNL $\underline{\text{R}}$ QKLLNGGGGGGGGGGGSMQIFVKTLTGK TTILEVPSDTIENVKAKIQDKEGIPPDQQRLIFAGKQLEDGRTLSDYNIQKESTLHLVLRGG	14581.4	14578.1 $\pm$ 1.1	NA
ubiquitin–NoxaBH3 (UP)	MGMQIFVKLTGKTTILEVPSDTIENVKAKIQDKEGIPPDQQRLIFAGKQLEDGRTLSDYNIQKESTLHLVLRGG GGGGGGGGGGGGSPADLKDEAA $\underline{\text{C}}$ LRIGDCVNL $\underline{\text{R}}$ QKLLNLEHHHHH	13540.3 <sup>c</sup>	13536.7 $\pm$ 0.5	NA
NoxaBH3–ubiquitin-K48R/ K63R (PU-KKmt)	MGSSHHHHSSGLVPRGSHMPADLKDEAA $\underline{\text{C}}$ LRIGDCVNL $\underline{\text{R}}$ QKLLNGGGGGGGGGGGSMQIFVKTLTGKTTIL EVEPSDTIENVKAKIQDKEGIPPDQQRLIFAGKQLEDGRTLSDYNIQKESTLHLVLRGG	14637.4 <sup>c</sup>	14636.6 $\pm$ 0.9	NA
NoxaBH3–ubiquitin-Bpy (PU-Bpy)	see above	14761.6	14760.1 $\pm$ 1.8	87
ubiquitin–NoxaBH3-Bpy (UP-Bpy)	see above	13720.5	13719.4 $\pm$ 0.4	80
NoxaBH3–ubiquitin-K48R/ K63R-Bpy (PU-KKmt-Bpy)	see above	14817.6	14816.0 $\pm$ 1.2	85

<sup>a</sup>Mass deconvolution was performed using ProMass. <sup>b</sup>Percent conversion was calculated by comparing the ion count of the cross-linked product to that of the starting material plus product. <sup>c</sup>Calculated mass for the conjugate with the N-terminal Met cleaved. NA, not applicable.



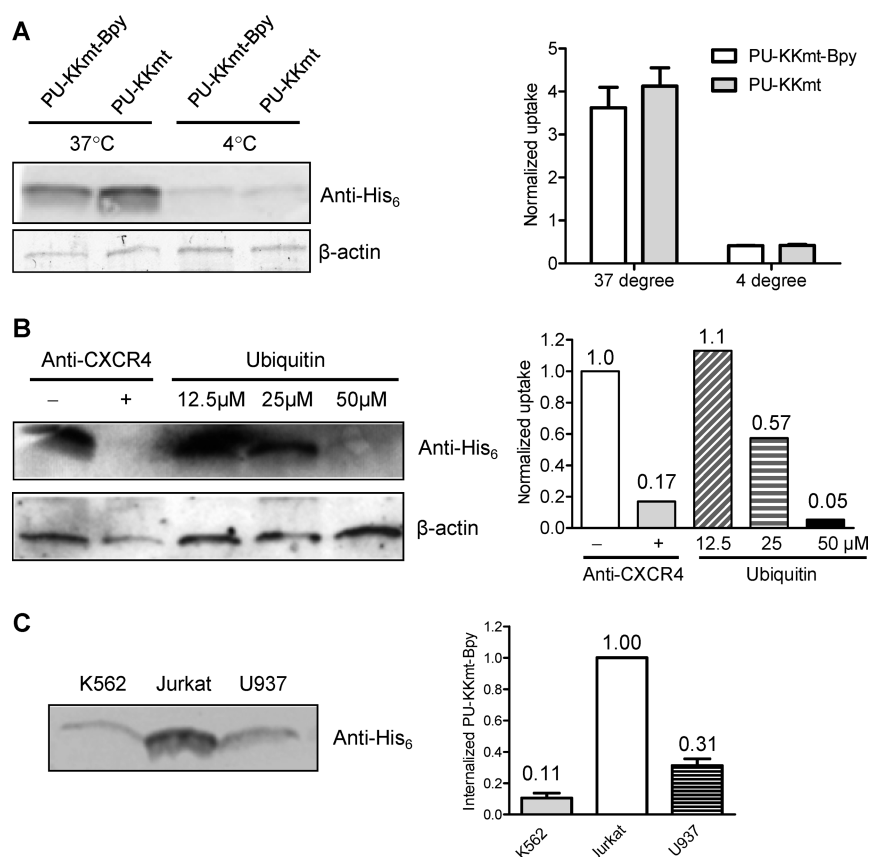


**Figure 4.** Uptake of ubiquitin–NoxaBH3 peptide conjugates is temperature- and CXCR4-dependent. (A) Western blot analysis of the uptake of PU-KKmt and PU-KKmt-Bpy into Jurkat cells at 37 or 4 °C. The relative uptakes were normalized over  $\beta$ -actin signal and plotted in the histogram. (B) Western blot analysis of the uptake of PU-KKmt-Bpy (0.5  $\mu$ M) into Jurkat cells at 37 °C after pretreating cells with the CXCR4 antibody (25  $\mu$ g/mL) or ubiquitin at concentrations of 12.5, 25, and 50  $\mu$ M. The intensities were quantified by densitometry, normalized over  $\beta$ -actin levels, and plotted in the histogram. (C) PU-KKmt-Bpy uptake at 37 °C is dependent on CXCR4 expression. K562, Jurkat, and U937 cells were incubated with 0.5  $\mu$ M PU-KKmt-Bpy for 2 h before cell lysis and Western blot analysis.

induces structural changes in the regions of Phe-4, Asp-58, and Val-70 that are involved in the ubiquitin binding to CXCR4, we prepared the [5%  $^{13}\text{C}$ ;  $U$ - $^{15}\text{N}$ ]-labeled PU-KKmt and PU-KKmt-Bpy conjugates and recorded 2D [ $^{15}\text{N}$ ,  $^1\text{H}$ ] HSQC spectra. The HSQC spectra of PU-KKmt and PU-KKmt-Bpy were then compared with that of the ubiquitin<sup>26</sup> (Figure 3). No significant alterations of polypeptide backbone  $^{15}\text{N}$  and  $^1\text{H}$  chemical shifts were registered upon cross-linking for residues implicated in ubiquitin binding to CXCR4; that is, signals arising from Phe-4, Asp-58, and Val-70 were not affected by the cross-linking (Figure 3). Overall, comparison of the HSQC spectra shows that peptide fusion as well as cross-linking did not affect the structure of the folded ubiquitin domain, particularly the regions implicated in binding to CXCR4.

**Uptake Mechanism of the Ubiquitin–Peptide Conjugates.** Since CXCR4-mediated endocytosis is energy-dependent and can be inhibited at low temperatures, we investigated the effect of switching the incubation temperature from 37 to 4 °C on the uptake of PU-KKmt and PU-KKmt-Bpy in the CXCR4-positive Jurkat cells. Because PU-KKmt and PU-KKmt-Bpy contain a His-tag at their N-termini, we measured the internalization of the conjugates by Western blot using an anti-His tag antibody. We observed >4-fold drop in the uptake for both after lowering the temperature to 4 °C (Figure 4A), indicating that the internalization was energy-dependent and that Bpy-cross-linking did not enhance uptake at either temperature. To confirm that the uptake is mediated through

CXCR4, we preincubated Jurkat cells with either anti-CXCR4 antibody or ubiquitin prior to PU-KKmt-Bpy treatment. We found that the pretreatment with anti-CXCR4 antibody led to an ~83% drop in the uptake, while the preincubation with ubiquitin resulted in a concentration-dependent decrease in the uptake (Figure 4B). These reductions are consistent with the CXCR4-mediated endocytosis mechanism as both anti-CXCR4 antibody and ubiquitin can block the ubiquitin binding site of CXCR4 on the Jurkat cell surface. The use of a large excess of ubiquitin appeared critical as the preincubation with 12.5  $\mu$ M ubiquitin did not inhibit the uptake (Figure 4B). Since the uptake depends on CXCR4, we evaluated how CXCR4 expression level affects uptake. We chose three cancer cell lines with the following CXCR4 expression order: Jurkat > U937 > K562<sup>27</sup> and incubated them with 0.5  $\mu$ M PU-KKmt-Bpy separately for 2 h. The internalization of PU-KKmt-Bpy was quantified by Western blot using anti-His tag antibody. To our satisfaction, Jurkat cells showed the highest uptake, while K562 cells showed the lowest (Figure 4C), indicating that indeed the uptake efficiency correlates with the CXCR4 expression level. Taken together, these results validated our hypothesis that ubiquitin can serve as a protein carrier for targeted delivery of anticancer agents such as the cross-linked peptides into the CXCR4-expressing cancer cells.

**Cellular Activities of the Ubiquitin–Peptide Conjugates.** To probe whether the ubiquitin–NoxaBH3 peptide conjugates can be released into the cytosol after CXCR4-mediated endocytosis and exhibit cell-killing activity, we

evaluated the cellular activities of PU-KKmt and PU-KKmt-Bpy. Thus, Jurkat, U937, and K562 cells were treated with PU-KKmt or PU-KKmt-Bpy at concentrations ranging from 100 to 2000 nM for 24 h, and the cell viability was assessed using the MTS assay. We found that while PU-KKmt showed no significant activities against all three cell lines, PU-KKmt-Bpy selectively killed nearly 50% Jurkat cells at 2  $\mu$ M (Figure 5). Since PU-KKmt and PU-KKmt-Bpy exhibited similar uptake at 37 °C (Figure 4A), the discrete activity of PU-KKmt-Bpy suggests that the higher inhibitory activity of

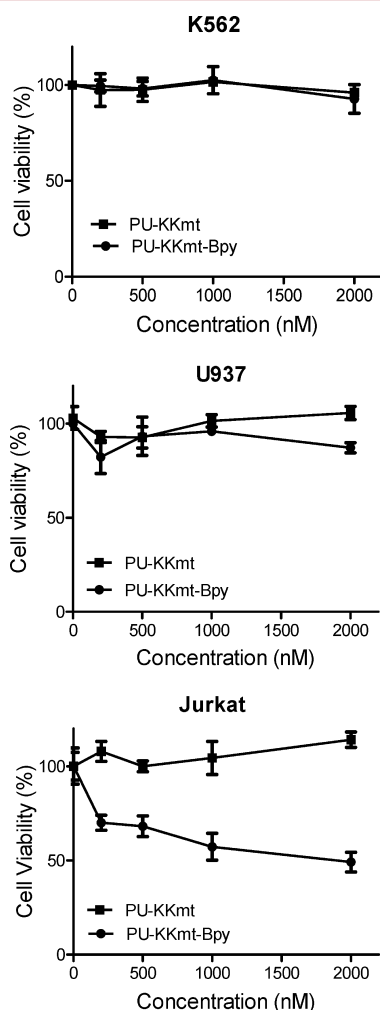


**Figure 5.** Cell-killing activities of PU-KKmt and PU-KKmt-Bpy against K562, U937, and Jurkat cells. The MTS-based cell viability assays were performed in triplicate, and the data were plotted as the mean  $\pm$  SD.

PU-KKmt-Bpy against Mcl-1 ( $K_i = 0.7 \pm 0.2$  nM) afforded by cross-linking is crucial for its cellular activity. Moreover, the lack of activities against K562 and U937 cells by PU-KKmt-Bpy emphasizes the importance of CXCR4 in mediating the uptake of these conjugates.

#### Serum Stability of the Ubiquitin–Peptide Conjugates.

Previously, we have shown that biaryl cross-linking greatly increased serum stability of the NoxaBH3 peptides.<sup>20</sup> To examine whether Bpy cross-linking with the ubiquitin–peptide conjugates has a similar effect, we incubated PU-KKmt and PU-KKmt-Bpy with fresh mouse serum and monitored the stability of the conjugates by ELISA using antiubiquitin or

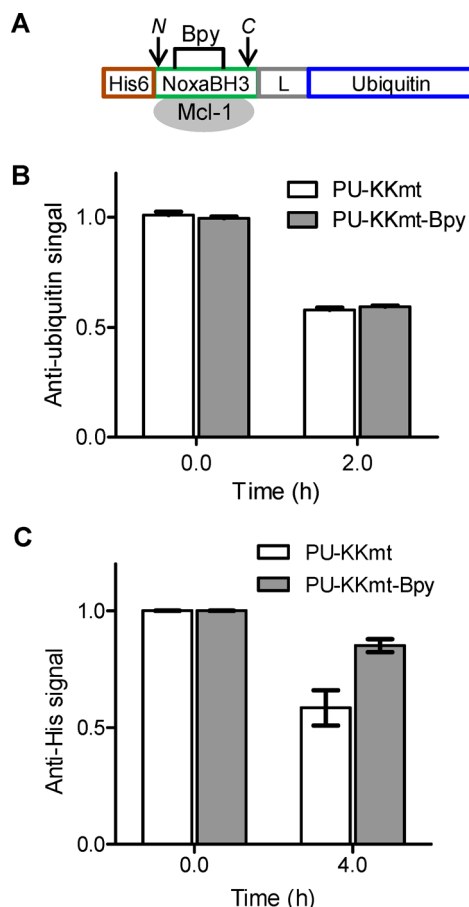


**Figure 6.** Bpy cross-linking stabilizes the N-terminus of the NoxaBH3 peptide in the ubiquitin conjugate. (A) Scheme for the ubiquitin–NoxaBH3 peptide constructs and their potential proteolytic sites. (B) ELISA signals as detected by antiubiquitin antibodies. (C) ELISA signals as detected by anti-His tag antibodies. ELISA assays were performed in duplicate, and the data were plotted as the mean  $\pm$  SD.

anti-His tag antibodies (Figure 6). Since the conjugate binding to Mcl-1-immobilized on the plate surface necessitates the intact peptide domain, the use of antiubiquitin and anti-His tag antibodies allows us to track the proteolytic stability of the C- and N-terminal regions of the NoxaBH3 peptide, respectively. Figure 6B shows that Bpy cross-linking had no effect on preventing the cleavage at the C-terminus of the NoxaBH3 after 2 h of incubation. Figure 6C shows that Bpy cross-linking significantly slowed down the proteolytic cleavage at the N-terminus of the NoxaBH3 domain. Taken together, these results indicate that the cross-linking stabilizes the N-terminal extension of the NoxaBH3 domain, a region closer to the chemical cross-linker, while exerting little effect on the more flexible linker region, similar to what was observed with the hydrocarbon-cross-linked peptides.<sup>28</sup>

Collectively, our data show that the extracellular ubiquitin identified recently as an endogenous ligand for CXCR4 can be harnessed as a conjugation partner for targeted delivery of the anticancer agents. Specifically, we explored the utility of ubiquitin in enhancing the intracellular delivery of the side-chain-cross-linked NoxaBH3 peptides, which were reported to have potent inhibitory activities against Mcl-1 but modest cellular activities because of the inefficient pinocytosis-based uptake.<sup>19</sup> Besides increased efficiency in uptake, the conjugation of ubiquitin also led to significant increases in inhibitory activity

as well as serum stability. This work provides a rare example of applying chemical cross-linkers directly onto intact proteins to reinforce their structure<sup>29</sup> and enhance their biological function. Compared with the use of extensive chemical modifications to optimize membrane permeation of the side-chain-cross-linked peptides,<sup>30</sup> the conjugation of ubiquitin, preferably at its N-terminus, with the peptide-based inhibitors represents a complementary approach and is particularly attractive for targeting tumor cells overexpressing the chemokine receptor CXCR4.

## CONCLUSIONS

In summary, we have demonstrated for the first time the use of ubiquitin as a conjugation partner for targeted delivery of the peptide-based inhibitors into CXCR4-positive cancer cells. Extending our earlier work on the distance-matching cross-linkers with peptides, we found that 6,6'-bis-bromomethyl-[3,3']bipyridine (Bpy) can be used to efficiently cross-link the ubiquitin-NoxaBH3 peptide conjugates containing two cysteines located at *i*, *i*+7 positions. The resulting Bpy-cross-linked ubiquitin-peptide conjugates exhibited higher inhibitory activity against Mcl-1, improved selective activity in CXCR4-expressing Jurkat cells, and increased proteolytic stability in peptide regions close to the cross-linking site. Mechanistic studies revealed that the ubiquitin/CXCR4 axis is crucial for the selective uptake of the ubiquitin-peptide conjugates. While this work focuses on targeted delivery of the NoxaBH3-peptide-based Mcl-1 inhibitors, it should be noted that other anticancer agents such as paclitaxel can be similarly conjugated to the N-terminus of ubiquitin for the targeted delivery into cancer cells to increase their therapeutic windows.

## AUTHOR INFORMATION

### Corresponding Author

\*E-mail: hwang3@hmc.psu.edu (H.W.); qinglin@buffalo.edu (Q.L.).

### Notes

The authors declare no competing financial interest.

## ACKNOWLEDGMENTS

We gratefully acknowledge the Pardee Foundation and Oishei Foundation (to Q.L.), the National Science Foundation (MCB 0817857 to T.S.), and the National Institutes of Health (CA 082197 to H.-G.W.) for financial support.

## REFERENCES

- (1) Craik, D. J., Fairlie, D. P., Liras, S., and Price, D. (2013) The future of peptide-based drugs. *Chem. Biol. Drug Des.* 81, 136–147.
- (2) Heitz, F., Morris, M. C., and Divita, G. (2009) Twenty years of cell-penetrating peptides: from molecular mechanisms to therapeutics. *Br. J. Pharmacol.* 157, 195–206.
- (3) Morris, M. C., Depollier, J., Mery, J., Heitz, F., and Divita, G. (2001) A peptide carrier for the delivery of biologically active proteins into mammalian cells. *Nat. Biotechnol.* 19, 1173–1176.
- (4) Henchey, L. K., Jochim, A. L., and Arora, P. S. (2008) Contemporary strategies for the stabilization of peptides in the  $\alpha$ -helical conformation. *Curr. Opin. Chem. Biol.* 12, 692–697.
- (5) Bock, J. E., Gavenonis, J., and Kritzer, J. A. (2012) Getting in shape: controlling peptide bioactivity and bioavailability using conformational constraints. *ACS Chem. Biol.* 8, 488–499.
- (6) Schafmeister, C. E., Po, J., and Verdine, G. L. (2000) An all-hydrocarbon cross-linking system for enhancing the helicity and metabolic stability of peptides. *J. Am. Chem. Soc.* 122, 5891–5892.

- (7) Schwarze, S. R., Ho, A., Vocero-Akbani, A., and Dowdy, S. F. (1999) In vivo protein transduction: delivery of a biologically active protein into the mouse. *Science* 285, 1569–1572.
- (8) Brown, C. J., Quah, S. T., Jong, J., Goh, A. M., Chiam, P. C., Khoo, K. H., Choong, M. L., Lee, M. A., Yurlova, L., Zolghadr, K., Joseph, T. L., Verma, C. S., and Lane, D. P. (2012) Stapled peptides with improved potency and specificity that activate p53. *ACS Chem. Biol.* 8, 506–512.
- (9) Saar, K., Lindgren, M., Hansen, M., Eiriksdóttir, E., Jiang, Y., Rosenthal-Aizman, K., Sassian, M., and Langel, Ü. (2005) Cell-penetrating peptides: a comparative membrane toxicity study. *Anal. Biochem.* 345, 55–65.
- (10) Burkhart, D. J., Kalet, B. T., Coleman, M. P., Post, G. C., and Koch, T. H. (2004) Doxorubicin-formaldehyde conjugates targeting  $\alpha v \beta 3$  integrin. *Mol. Cancer Ther.* 3, 1593–1604.
- (11) Widera, A., Norouziyan, F., and Shen, W. C. (2003) Mechanisms of TfR-mediated transcytosis and sorting in epithelial cells and applications toward drug delivery. *Adv. Drug Delivery Rev.* 55, 1439–1466.
- (12) Garnett, M. C. (2001) Targeted drug conjugates: principles and progress. *Adv. Drug Delivery Rev.* 53, 171–216.
- (13) Saini, V., Marchese, A., and Majetschak, M. (2010) CXC chemokine receptor 4 is a cell surface receptor for extracellular ubiquitin. *J. Biol. Chem.* 285, 15566–15576.
- (14) Majetschak, M., Krehmeier, U., Bardenheuer, M., Denz, C., Quintel, M., Voggenreiter, G., and Obertacke, U. (2003) Extracellular ubiquitin inhibits the TNF-alpha response to endotoxin in peripheral blood mononuclear cells and regulates endotoxin hyporesponsiveness in critical illness. *Blood* 101, 1882–1890.
- (15) Majetschak, M., Ponelies, N., and Hirsch, T. (2006) Targeting the monocytic ubiquitin system with extracellular ubiquitin. *Immunol. Cell Biol.* 84, 59–65.
- (16) Balkwill, F. (2004) The significance of cancer cell expression of the chemokine receptor CXCR4. *Semin. Cancer Biol.* 14, 171–179.
- (17) Sun, Y. X., Wang, J., Shelburne, C. E., Lopatin, D. E., Chinnaiyan, A. M., Rubin, M. A., Pienta, K. J., and Taichman, R. S. (2003) Expression of CXCR4 and CXCL12 (SDF-1) in human prostate cancers (PCa) in vivo. *J. Cell Biochem.* 89, 462–473.
- (18) Daino, H., Matsumura, I., Takada, K., Odajima, J., Tanaka, H., Ueda, S., Shibayama, H., Ikeda, H., Hibi, M., Machii, T., Hirano, T., and Kanakura, Y. (2000) Induction of apoptosis by extracellular ubiquitin in human hematopoietic cells: possible involvement of STAT3 degradation by proteasome pathway in interleukin 6-dependent hematopoietic cells. *Blood* 95, 2577–2585.
- (19) Muppidi, A., Wang, Z., Li, X., Chen, J., and Lin, Q. (2011) Achieving cell penetration with distance-matching cysteine cross-linkers: a facile route to cell-permeable peptide dual inhibitors of Mdm2/Mdmx. *Chem. Commun.* 47, 9396–9398.
- (20) Muppidi, A., Doi, K., Edwardraja, S., Drake, E. J., Gulick, A. M., Wang, H.-G., and Lin, Q. (2012) Rational design of proteolytically stable, cell-permeable peptide-based selective Mcl-1 inhibitors. *J. Am. Chem. Soc.* 134, 14734–14737.
- (21) Guntert, P., Dotsch, V., Wider, G., and Wuthrich, K. (1992) Processing of multidimensional NMR data with the new software PROSA. *J. Biomol. NMR* 2, 619–629.
- (22) Keller, R. (2004) The Computer Aided Resonance Assignment Tutorial. CANTINA Verlag.
- (23) Richard, J. P., Melikov, K., Vives, E., Ramos, C., Verbeure, B., Gait, M. J., Chernomordik, L. V., and Lebleu, B. (2003) Cell-penetrating peptides: a reevaluation of the mechanism of cellular uptake. *J. Biol. Chem.* 278, 585–590.
- (24) Ye, Y., and Rape, M. (2009) Building ubiquitin chains: E2 enzymes at work. *Nat. Rev. Mol. Cell Biol.* 10, 755–764.
- (25) Saini, V., Marchese, A., Tang, W.-J., and Majetschak, M. (2011) Structural determinants of ubiquitin-CXC chemokine receptor 4 interaction. *J. Biol. Chem.* 286, 44145–44152.
- (26) Jaravine, V. A., Zhuravleva, A. V., Permi, P., Ibraghimov, I., and Orekhov, V. Y. (2008) Hyperdimensional NMR spectroscopy with nonlinear sampling. *J. Am. Chem. Soc.* 130, 3927–3936.



(27) Zeng, Z., Samudio, I. J., Munsell, M., An, J., Huang, Z., Estey, E., Andreeff, M., and Konopleva, M. (2006) Inhibition of CXCR4 with the novel RCP168 peptide overcomes stroma-mediated chemoresistance in chronic and acute leukemias. *Mol. Cancer Ther.* 5, 3113–3121.

(28) Bird, G. H., Madani, N., Perry, A. F., Princiotta, A. M., Supko, J. G., He, X., Gavathiotis, E., Sodroski, J. G., and Walensky, L. D. (2010) Hydrocarbon double-stapling remedies the proteolytic instability of a lengthy peptide therapeutic. *Proc. Natl. Acad. Sci. U.S.A.* 107, 14093–14098.

(29) Zhang, F., Sadovski, O., Xin, S. J., and Woolley, G. A. (2007) Stabilization of folded peptide and protein structures via distance matching with a long, rigid cross-linker. *J. Am. Chem. Soc.* 129, 14154–14155.

(30) Chang, Y. S., Graves, B., Guerlavais, V., Tovar, C., Packman, K., To, K. H., Olson, K. A., Kesavan, K., Gangurde, P., Mukherjee, A., Baker, T., Darlak, K., Elkin, C., Filipovic, Z., Qureshi, F. Z., Cai, H., Berry, P., Feyfant, E., Shi, X. E., Horstick, J., Annis, D. A., Manning, A. M., Fotouhi, N., Nash, H., Vassilev, L. T., and Sawyer, T. K. (2013) Stapled alpha-helical peptide drug development: a potent dual inhibitor of MDM2 and MDMX for p53-dependent cancer therapy. *Proc. Natl. Acad. Sci. U.S.A.* 110, E3445–3454.

(31) Czabotar, P. E., Lee, E. F., van Delft, M. F., Day, C. L., Smith, B. J., Huang, D. C., Fairlie, W. D., Hinds, M. G., and Colman, P. M. (2007) Structural insights into the degradation of Mcl-1 induced by BH3 domains. *Proc. Natl. Acad. Sci. U.S.A.* 104, 6217–6222.